American Journal of Sciences and Engineering Research

E-ISSN -2348 – 703X, Volume 6, Issue 2, 2023

Effect of Storage Tank Geometry on Liquefied Natural Gas Boil-off Gas Production

Victor Joseph AIMIKHE[1], Majid Abiodun ADEYEMI[2]

[1]*Department of Petroleum and Gas Engineering, University of Port Harcourt, Nigeria*

[2]*Department of Construction and Drilling, Saudi Petroleum Services Polytechnic (SPSS) Dammam, Saudi Arabia.*

Abstract: *Liquefied natural gas (LNG) is usually stored in specialized storage tanks and conveyed to regions where it is required. During storage, some LNG vaporizes into gaseous state within the tanks, thereby increasing the tank pressure and posing environmental risks when vented. Therefore, minimizing the produced boil-off gas is imperative. Numerous studies have modeled the boil-off gas rate from LNG storage tanks. However, studies comparing different tank geometries for ascertaining the tank type with the least produced boil-off gas are scarce in the open literature. This study analyzed three commonly used LNG storage tank geometries including the prismatic, spherical, and cylindrical tanks. Fourier and Newton's laws of conduction and convection, coupled with nucleate boiling, were used to estimate the produced boil-off gas using similar LNG and tank properties. The results showed that the cylindrical tank had the least boil-off gas rates compared to the spherical and prismatic tanks.*

Keywords: *LNG, Boil-off gas, LNG storage tanks, LNG modeling.*

I. Introduction

The clamor for a sustainable energy future and transition has increased the spotlight on natural gas due to its characteristically lower emission levels compared to other fossil fuels. Switching from other fossil fuels like coal and oil to natural gas to reduce greenhouse gas (GHG) emissions will be critical to a clean energy transition [1]. The strict environmental and government policies in mitigating GHG emissions in many industries globally have also enhanced using natural gas as an alternative fuel. For instance, natural gas-powered vessels are gaining more attention in the maritime sector than conventional heavy fuel oil or marine diesel oil. Gas-fired power plants are increasingly becoming a more environmentally sustainable way of electricity generation compared to their coal-fired counterparts. Likewise, natural gas utilization as automobile fuels has seen the number of gas-powered vehicles grow to around twenty-three million globally [2]. Also, natural gas demand growth has been recorded in the fertilizer, petrochemical, chemical intermediates, etc. industries. Consequently, the demand for natural gas has been projected to grow rapidly to 768 bcm by 2040 from 136 in 2000 [3]. This rapid demand for natural gas translates to an increased supply of the commodity to many regions around the globe.

LNG and pipeline transport are the two most popular methods of transporting natural gas. For long-distance transportation, LNG becomes the more cost-effective and favorable transportation choice. The transportation is usually done by ship due to the high volume ratio (600 times) of gas to the liquid phase at –163 ^{o}C [4], [5]. However, while transporting the bulk LNG fluid in special tanks, also known as thermoses, there is always a tendency for vaporization due to heat ingress created by the ambient and LNG temperature

 Received-18-03-2023, Accepted- 28-03-2023

gradient. This vaporized portion of the LNG into the gaseous phase is known as boil-off gas –BOG [6]. The BOG increases the tank pressure leading to unsafe internal tank pressures. It also reduces the quality of the LNG and has been identified as a super source of fugitive methane emissions [7]. To maintain the tank pressure within the safe range, BOG should be continuously eliminated. Conventionally, the BOG is vented (an environmentally unsafe practice), utilized as fuel, burned in a gasification unit, or re-liquefied and sent back into the LNG tank. In cases where the BOG cannot be used as fuel, the environmentally unsafe option of venting or the expensive option of re-liquefaction is undertaken.

Furthermore, the more volatile components (nitrogen and methane) boil off first, changing LNG composition and quality over time. This phenomenon, known as aging, is critical in the LNG trade since LNG is sold depending on its energy content. Hence, it is imperative to determine the amount of BOG anticipated for an efficient loading, unloading, and storage tank systems design.

Many researchers have studied BOG production from various LNG storage tanks [5], [8-15]. However, studies on LNG storage tank geometry's effect on produced BOG are limited in published literature. Minimizing produced BOG will reduce costs and the adverse impact of its production on the environment. Therefore this study aims to determine the effect of three tank geometries (prismatic, spherical, and cylindrical) on the produced BOG.

II. Materials and Methods

This study utilizes the principles of heat transfer by conduction (Fourier's law) and convection (Newton's law of cooling) to model heat transfers across the various tank geometries. Figures 1 and 2 show the tank shapes considered in this study. The total heat ingress is considered across the entire surface area of the various tank geometries. Furthermore, the nucleate boiling of the LNG in the tank internals is also considered. Data for the numerical analysis are given in the appendix.

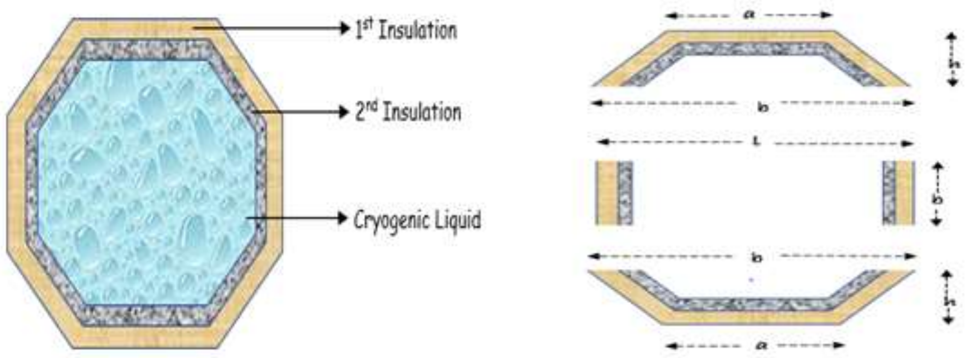

Fig. 1. Prismatic tank shape showing the cross-sections

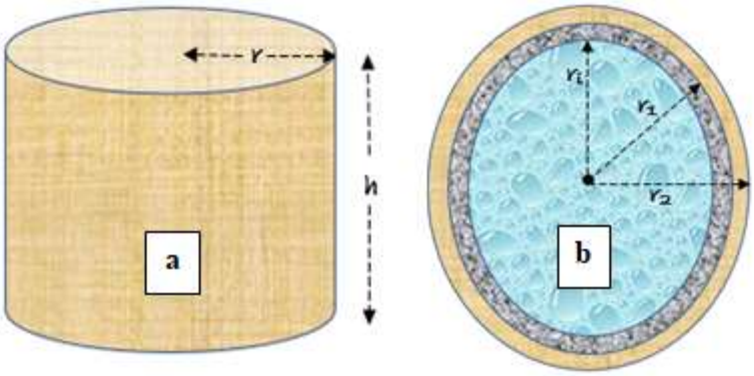

Fig. 2. (a) Cylindrical (b) Spherical tank shapes

The total inner heat transfer coefficient that accounts for nucleate boiling is given as follows:

$$h_{nb} = 0.00122 \frac{\Delta T^{0.24} \Delta P^{0.75} {C_{pl}}^{0.45} {\rho_l}^{0.49} {k_l}^{0.79}}{\sigma^{0.5} {h_{fg}}^{0.24} {\mu_l}^{0.29} {\rho_g}^{0.24}} \tag{1}$$

Where, C_{pl} = LNG heat of vaporization$[J/kgK]$, μ_g= Viscosity of Methane gas at -162°C $[cp]$, ρ_l = LNG density$[Kg/m^3]$, k_l = LNG thermal conductivity$[W/mK]$, μ_l = LNG viscosity at -162 °C$[Ns/m]$, ρ_g = Density of methane gas at -162 °C$[Kg/m^3]$, ρ_g = Density of methane gas at -162°C$[Kg/m^3]$, h_{fg} = LNG latent heat of vaporization$[J/Kg^3]$, σ = Surface tension between LNG and boil-off gas$[J/m^2]$, ΔT = Temperature difference between wall, $T_{wall} - T_{sat}$ [°C], ΔP = Pressure difference between wall, $P_{wall} - P_{sat}$ $[bar]$

An enhancement factor, F, is determined to account for the increased contribution of convective heat transfer. Likewise, a suppression factor, S, accounts for the partially suppressed nucleate heat boiling. The enhancement factor F, used in this study, is given as follows:

$$F = 2.35 \left(\frac{1}{X_{tt}} + 0.213\right)^{0.736} \tag{2}$$

Where

X_{tt}, Martinelli parameter is given as

$$X_{tt} = \left(\frac{1-x}{x}\right)^{0.99} \left(\frac{\rho_g}{\rho_l}\right)^{0.5} \left(\frac{\mu_l}{\mu_g}\right)^{0.1} \tag{3}$$

And x, is the vapor quality/ dryness fraction given as:

$$x = \frac{-C_{pl}(T_s - T_i)}{h_{fg}} \tag{4}$$

The suppression factor, S, is given as:

$$S = \left(\frac{1}{1 + 2.53 \times 10^{-6} (Re_l F^{1.25})^{1.17}}\right) \tag{5}$$

Where

Re_l, is the Reynolds number expressed as:

$$Re_l = \frac{C_{pl}\mu_l}{k_l} \tag{6}$$

Where, μ_g = Viscosity of Methane gas at -162°C$[Ns/m]$, μ_l = LNG viscosity at -162°C$[Ns/m]$, ρ_g = Density of methane gas at -162°C$[Kg/m^3]$, ρ_l = LNG density$[Kg/m^3]$, T_s = Saturation temperature of LNG[°C], T_i = Bulk temperature of LNG [°C]

Therefore, the overall heat convection coefficient expression that accounts for the enhancement and suppression factors is given as:

$$h = (S \times h_{nb}) + (F \times h_{cb}) \tag{7}$$

Note: $h_{cb} = h_i$

Therefore, for a spherical tank system, the total heat transfer can be expressed as:

$$T_i - T_\infty = -\frac{Q}{4\pi}\left[\frac{1}{hr_i^2} + \frac{1}{k_1}\left(\frac{1}{r_i} - \frac{1}{r_1}\right) + \frac{1}{k_2}\left(\frac{1}{r_1} - \frac{1}{r_2}\right) + \frac{1}{k_3}\left(\frac{1}{r_2} - \frac{1}{r_3}\right) + \frac{1}{k_4}\left(\frac{1}{r_3} - \frac{1}{r_o}\right) + \frac{1}{h_o r_o^2}\right] \tag{8}$$

Substituting equation 7 into 8 gives:

$$Q = \frac{-4\pi(T_i - T_\infty)}{\left[\frac{1}{(F \times h_i) + S\left(0.00122\frac{\Delta T^{0.24}\Delta P^{0.75}C_{pl}{}^{0.45}\rho_l{}^{0.49}k_l{}^{0.79}}{\sigma^{0.5}h_{fg}{}^{0.24}\mu_l{}^{0.29}\rho_g{}^{0.24}}\right)r_i^2} + \frac{1}{k_1}\left(\frac{1}{r_i} - \frac{1}{r_1}\right) + \cdots + \frac{1}{k_2}\left(\frac{1}{r_1} - \frac{1}{r_2}\right) + \frac{1}{k_3}\left(\frac{1}{r_2} - \frac{1}{r_3}\right) + \frac{1}{k_4}\left(\frac{1}{r_3} - \frac{1}{r_o}\right) + \frac{1}{h_o r_o^2}\right]} \tag{9}$$

Likewise, the total heat ingress across a linear tank system is:

$$T_\infty - T_i = \frac{Q}{A}\left(\frac{1}{h} + \frac{\Delta x_1}{k_1} + \frac{\Delta x_2}{k_2} + \frac{\Delta x_3}{k_3} + \frac{\Delta x_4}{k_4} + \frac{\Delta x_5}{k_5} + \frac{\Delta x_6}{k_6} + \frac{1}{h_o}\right) \tag{10}$$

Substituting equation 7 into 10 gives:

$$Q = \frac{T_\infty - T_i}{\frac{1}{A}\left[\frac{1}{(F \times h_i) + S\left(0.00122\frac{\Delta T^{0.24}\Delta P^{0.75}C_{pl}{}^{0.45}\rho_l{}^{0.49}k_l{}^{0.79}}{\sigma^{0.5}h_{fg}{}^{0.24}\mu_l{}^{0.29}\rho_g{}^{0.24}}\right)} + \frac{\Delta x_1}{k_1} + \frac{\Delta x_2}{k_2} + + \frac{\Delta x_3}{k_3} + \frac{\Delta x_4}{k_4} + \frac{\Delta x_5}{k_5} + \frac{\Delta x_6}{k_6} + \frac{1}{h_o}\right]} \tag{11}$$

To account for the total surface area, A of the linear systems, which applies to prismatic tanks, the authors developed and used the correlation in equation 12.

$$A = -2.058E(-7)V^2 + 0.1781V + 1895 \;\; [m^2] \tag{12}$$

Where, V = Tank volume (m^3).

For a Cylindrical tank system, the total heat ingress is expressed as:

$$T_i - T_\infty = -\frac{Q}{2\pi r_o L}\left[\frac{r_o}{r_i h} + \frac{r_o}{k_1} ln\frac{r_1}{r_i} + \frac{r_o}{k_2} ln\frac{r_2}{r_1} + \frac{r_o}{k_3} ln\frac{r_3}{r_2} + \frac{r_o}{k_4} ln\frac{r_o}{r_3} + \frac{1}{h_o}\right] \quad (13)$$

Substituting equation 7 into 13 gives:

$$Q = \frac{-2\pi r_o L(T_i - T_\infty)}{\left[\frac{1}{(F \times h_i) + S\left(0.00122\frac{\Delta T^{0.24}\Delta P^{0.75}{C_{pl}}^{0.45}{\rho_l}^{0.49}{k_l}^{0.79}}{\sigma^{0.5}{h_{fg}}^{0.24}{\mu_l}^{0.29}{\rho_g}^{0.24}}\right)r_i} + \frac{r_o}{r_i h} + \frac{r_o}{k_1} ln\frac{r_1}{r_i} + \frac{r_o}{k_2} ln\frac{r_2}{r_i} + \frac{r_o}{k_3} ln\frac{r_3}{r_2} + \frac{r_o}{k_4} ln\frac{r_o}{r_3} + \frac{1}{h_o}\right]} \quad (14)$$

Where Q = heat transfer rate (Watts), T_∞ = Ambient temperature (^{o}C), L = Length or Height of cylinder (meters), r = tank radius (meters), k = thermal conductivity (Wm^{-1}C^{-1}), x = material thickness (meters), h_o = outer heat transfer coefficient (Wm^{2} ^{o}C)

Equations 9, 11, and 14 were used to estimate the total heat transfer rate from the tank shapes under investigation. The boil-off gas produced per day for each tank geometry was calculated from the equation:

$$\text{BOG}(m^3) = \frac{Total\ Heat\ Transfer, Q}{Latent\ Heat\ of\ Vaporization, \times\ LNG\ Density} \times 3600 \times 24 \quad (15)$$

The LNG and tank parameters and the parameters associated with nucleate heat transfer coefficient, used for the analysis in this study, are given in Tables A1 and A2 of the Appendix, respectively.

III. Results and Discussion

Figure 3 shows the relationship between the percentage boil-off gas rate for each tank geometry and volume, considered. From the table, it can be seen that the rate of LNG boil-off is inversely proportional to tank volume. That is, the boil-off gas rate percent by volume is highest at smaller tank volumes and decreases as tank volumes increase. This reduction in boil-off gas rate as tank volume increases is because the heat transfer rate of small pressurized tanks is greater than that of large tanks due to the larger surface area to volume ratio of smaller tanks [8], [11]. Since the boil-off rate is directly proportional to the heat transfer rate, the boil-off gas rate by volume for smaller tanks is greater than that of larger tanks. Furthermore, the figure shows that prismatic tanks' boil-off gas rate is the largest. Cylindrical tanks have the least boil-off gas rate compared to spherical and prismatic tanks. This relatively low boil-off gas rate can be further reduced if the tank height is reduced optimally.

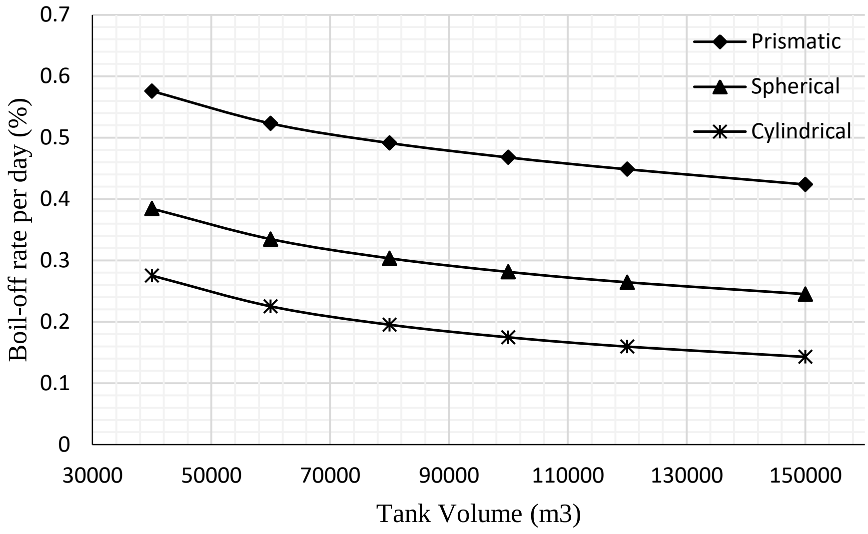

Fig. 3. Percentage boil-off gas rate versus tank volume

Figure 4 shows the relationship between boil-off gas produced and tank volumes of the prismatic, spherical, and cylindrical tank geometries. The figure shows that produced boil-off gas is directly proportional to tank volume. The rate at which the LNG is boiled off increases as the tank volume increases. This trend is because, as the tank volume increases, its total surface area also increases. An increase in the surface area will increase the heat transfer rate based on Fourier and Newton's laws of conduction and convection. Consequently, the boil-off gas produced increases. The figure further indicates that the boil-off gas produced is higher for prismatic tanks than for spherical and cylindrical tanks.

Figure 5 shows the relationship between produced boil-off gas and ambient temperatures, and from the figure, produced boil-off gas increases as the ambient temperature increases.

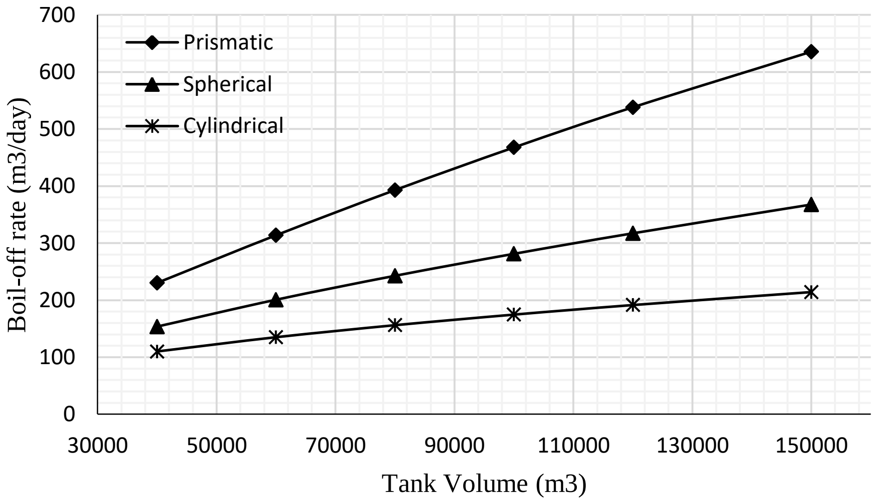

Fig. 4. Produced boil-off gas versus tank volume

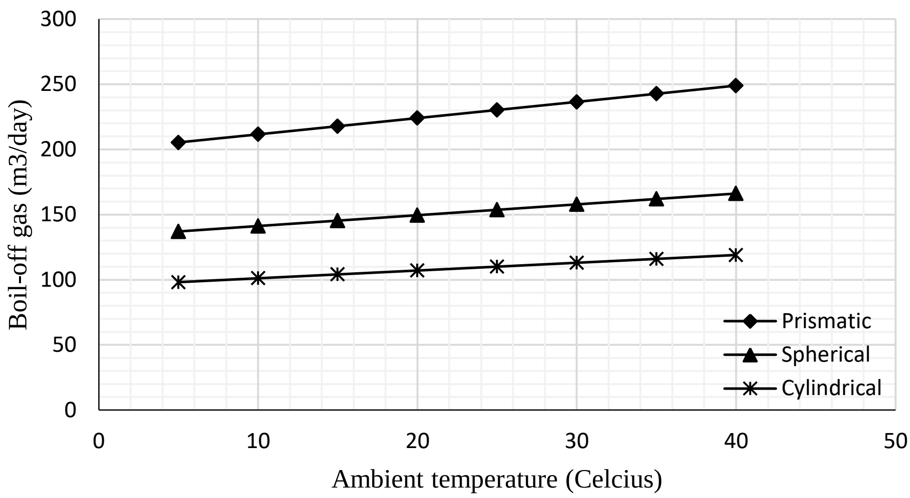

Fig. 5. Produced boil-off gas versus ambient temperature

The increase in the produced boil-off gas is due to the direct dependence of change in temperature on the heat transfer rate according to Fourier and Newton's laws of conduction and convection. Hence, the temperature change between ambiance and LNG in the tank increases as ambient temperatures increase. Therefore, the boil-off gas increases. This increase in boil-off gas as ambient temperatures increase agrees with the works of Zakaria et al. [5] and Wlodek [6]. The results further show that the cylindrical tank produced the least boil-off gas compared to the spherical and prismatic tanks.

The results of this study provide a template for LNG tank geometry selection for minimizing boil-off gas production. From the analysis of the results, the cylindrical tanks produce the least boil-off gas. The implication is that cylindrical LNG tanks are best suited for LNG carriers, automobile vehicles and trucks, and in base load or peak shaving LNG storage plants if the goal is to minimize boil-off gas production.

IV. Conclusion

This study compared the boil-off gas rates from three commonly used LNG storage tanks. They include prismatic, spherical, and cylindrical tanks. The comparison was made to ascertain the tank type with the potential to minimize the produced boil-off gas. For effective comparison, similar tank and LNG properties were used. From this study, the following conclusions can be reached.

(a) Percentage LNG boil-off gas rate by volume increases with decreasing tank volume.

(b) Produced boil-off gas increases with increasing tank volume

(c) Produced boil-off gas increases with rising ambient temperatures

(d) The cylindrical tank geometry produces the least boil-off gas, followed by the spherical tanks. The prismatic tanks had the highest-produced boil-off gas.

V. References

1. Marcogaz (2021). Liquefied Natural Gas As Transportation Fuel. Available at https://www.marcogaz.org/wp-content/uploads/2021/06/LNG-as-transportation-fuel.pdf.
2. US Department of Energy (2022). Alternative fuels data center. Natural gas vehicles. Available at https://afdc.energy.gov/vehicles/natural_gas.html.
3. IEA World Energy Outlook (2019). Analysis-IEA; International Energy Agency: Paris, France,
4. Khan MS, Qyyum MA, Ali W, Wazwaz A, Ansari KB, Lee M. (2020). Energy Saving through Efficient BOG Prediction and Impact of Static Boil-off-Rate in Full Containment-Type LNG Storage Tank. Energies 2020, 13, 5578; doi:10.3390/en13215578.

5. Zakaria MS, Osman K, Yusof AA, Hanafi MH, Saadun MN, Manaf MZ (2014). Parametric Analysis on Boil-off Gas Rate inside Liquefied Natural Gas Storage Tank. Journal of Mechanical Engineering and Sciences (JMES). 6, 845-853.
6. Włodek T. (2019). Analysis of boil-off rate problem in Liquefied Natural Gas (LNG) receiving terminals. 2nd International Conference on the Sustainable Energy and Environmental Development IOP Conf. Ser. Earth Environ. Sci. 214, 012105. doi:10.1088/1755-1315/214/1/012105.
7. Brandt AR, Heath GA, Kort EA, Sullivan F, Pétron G, Jordaan SM, Tans P, Wilcox J, Gopstein AM, Arent D, Wofsy S, Brown NJ, Bradley R, Stucky GD, Eardley D, Harriss R. (2014). Methane leaks from North American natural gas systems. Science. 343(6172):733-735
8. Adom E, Islam SZ, Ji X (2010). Modeling of Boil-off Gas in LNG tanks: A case study. Int. J. Eng. Technol. 2, 292–296.
9. Aimikhe, V.J (2011). Predicting Critical Internal Diameters of Onshore LNG Storage Tanks for Minimizing Boil-off Gas Production. Refereed Proceedings, SPE 150796. Annual International Conference of the SPE Nigeria Council, Abuja, Nigeria.
10. Aimikhe VJ, Kinigoma BS, Iyagba ET (2013). Predicting the Produced Boil-off Gas in a Moss Spherical LNG Vessel. Refereed Proceedings, SPE 167591. Annual International Conference of the SPE Nigeria Council, Lagos, Nigeria.
11. Lee DH, Cha SJ, Kim JD, Kim JH, Kim SK, Lee JM. (2021). Practical Prediction of the Boil-Off Rate of Independent-Type Storage Tanks. J. Mar. Sci. Eng. 9, 36. https://doi.org/10.3390/jmse9010036
12. Jeong H, Shim WJ (2017). Calculation of Boil-off Gas Generation of KC-1 membrane LNG Tank with High-Density Rigid Polyurethane Foam by Numerical Analysis.
13. Duan Z, Xue H, Gong X, Tang W. (2021). A thermal non-equilibrium model for predicting LNG boil-off in storage tanks incorporating the natural convection effect. Energy, 233. https://doi.org/10.1016/j.energy.2021.121162.
14. Kalikatzarakis M, Theotokatos G, Coraddu A, Sayan P, Wong SW (2022). Model-based analysis of the boil-off gas management and control for LNG fuelled vessels. Energy 251, 123872. https://doi.org/10.1016/j.energy.2022.123872.

Appendix

Table A1: Parameters for BOG modeling

LNG and Tank Parameters	
Outer Shell (Carbon steel) thickness (inches)	6
Inner Shell (9% Ni steel) thickness (inches)	9
Perlite Thickness (cm)	5
Polyurethane Thickness (cm)	3
Outer Heat Transfer Coefficient(W/m^2 °C)	80
Inner shell thermal conductivity, ki (W/m °C)	90.9
Perlite thermal conductivity, k2 (W/m °C)	0.038
Polyurethane thermal conductivity, k3 (W/m °C)	0.021
Outer shell thermal conductivity, ko (W/m °C)	35
LNG bulk temperature T (°C)	-160
Ambient temperature $\boldsymbol{T}_\infty$ (°C)	25
LNG Latent Heat (J/m^3)	198401912
Density of Methane gas, ρg (kg/m^3)	1.8104
Density of LNG, ρ_L (kg/m^3)	470
Viscosity of LNG, μ_L (cp)	0.146
Viscosity of Methane gas, μ_g (cp)	0.004526
Specific heat capacity of LNG, C_{pl} (J/kg °C)	2260

Latent heat of Evaporation, h_{fg} *(J/Kg)*	510000
Surface tension of LNG, σ (*N*/m^2)	0.014
Thermal heat coefficient, k_L (*W/mk*)	0.035

Table A2: Parameters associated with nucleate heat transfer coefficient

Vapor quality, $\boldsymbol{x}$	0.00657
Martinelli Parameter, $\boldsymbol{X_{tt}}$	8.048
Enhancement Factor, $\boldsymbol{F}$	1.056
Reynolds Number, $\boldsymbol{Re_l}$	9.427
Suppression Factor, $\boldsymbol{S}$	0.9999
Nucleate heat transfer coefficient, $\boldsymbol{h_{nb}}(\boldsymbol{W/m^2}℃)$	310.357
Inner heat transfer coefficient $\boldsymbol{h}$, $(\boldsymbol{W/m^2}℃)$ considering nucleate heat coefficient	363.13